# Low temperature heat capacity of $Fe_{1-x}Ga_x$ alloys with large magnetostriction

J. M. Hill
*Institute for Physical Research and Technology, Iowa State University, Ames, Iowa 50011, USA*

R. J. McQueeney*
*Department of Physics and Astronomy and Ames Laboratory, Iowa State University, Ames, Iowa 50011, USA*

Ruqian Wu
*Department of Physics and Astronomy, University of California, Irvine, California 92697, USA*

K. Dennis, R. W. McCallum, M. Huang, and T. A. Lograsso
*Ames Laboratory, Ames, Iowa 50011, USA*

(Received 14 August 2007; revised manuscript received 25 October 2007; published 22 January 2008)

The low temperature heat capacity $C_p$ of $Fe_{1-x}Ga_x$ alloys with large magnetostriction has been investigated. The data were analyzed in the standard way using electron ($\gamma T$) and phonon ($\beta T^3$) contributions. The Debye temperature $\Theta_D$ decreases approximately linearly with increasing Ga concentration, consistent with previous resonant ultrasound measurements and measured phonon dispersion curves. Calculations of $\Theta_D$ from lattice dynamical models and from measured elastic constants $C_{11}$, $C_{12}$, and $C_{44}$ are in agreement with the measured data. The linear coefficient of electronic specific heat $\gamma$ remains relatively constant as the Ga concentration increases, despite the fact that the magnetoelastic coupling increases. Band structure calculations show that this is due to the compensation of majority and minority spin states at the Fermi level.

DOI: 10.1103/PhysRevB.77.014430 PACS number(s): 75.80.+q, 65.40.Ba, 62.20.D−, 71.15.Mb

## I. INTRODUCTION

$Fe_{1-x}Ga_x$ alloys are known for their large magnetostriction. Values of the tetragonal magnetostriction coefficient, $\frac{3}{2}\lambda_{100}$, can reach values as high as ~400 ppm for certain alloy compositions and heat treatments.[1–3] The sharp rise in the magnetostriction near 19 at. % Ga composition can be explained by a simultaneously increasing magnetoelastic coupling $b_1$ and decreasing tetragonal shear modulus $C'$.[1] The decrease in $C'$ has been independently measured via resonant ultrasound techniques[1,4–6] and neutron scattering.[7] However, the nature and characterization of the large increase in magnetoelastic coupling with composition has been difficult to determine. It has been suggested that the increase in $b_1$ is related to short-range ordered clustering of the Ga atoms prior to the formation of long-range ordered structures near 19 at. % Ga.[8] Below ~19% Ga, $Fe_{1-x}Ga_x$ alloys are disordered and crystallize in a body-centered-cubic ($bcc$) $\alpha$-Fe ($A2$) structure. Above this composition, two ordered phases are possible: $D0_3$ and $B_2$. For itinerant magnetic alloys without significant short-range ordering (local) effects, $b_1$ depends on the spin-orbit coupling of electrons near the Fermi level. In strongly ferromagnetic alloys, the compositional dependence of the minority spin electronic density of states (DOS) at the Fermi level, $n_\downarrow(\varepsilon_F)$, can be related to magnetostriction.[9] Measurements of the linear coefficient of the electronic specific heat at low temperatures, $\gamma$ (also called the Sommerfeld constant) are directly proportional to the total electronic DOS at the Fermi level, $n(\varepsilon_F)$, and can be used to characterize the origins of magnetostriction. This is most clearly demonstrated in Ni-Fe alloys, where the zero magnetostriction composition (Permalloy) corresponds to a full majority spin band and a minimum in $n_\downarrow(\varepsilon_F)$ leading to a minimum in $\gamma$, as predicted in the "split-band model" of Berger.[9] We have undertaken a study of the low temperature heat capacity of Fe-Ga alloys to determine if variations in $\gamma$ are present that can be correlated with the large increase in magnetostriction. In addition, the lattice contribution to the specific heat, characterized by the Debye temperature $\Theta_D$, indicates strong lattice softening with added Ga in agreement with ultrasound and neutron scattering data.

## II. SAMPLE PREPARATION

Single crystal alloys of $Fe_{1-x}Ga_x$ were grown by the Bridgman technique (see Ref. 2 for more details of sample preparation). Gallium (99.999% pure) and electrolytic iron (99.99% pure) were cleaned and arc-melted together several times under an argon atmosphere. To prepare single crystal samples, the as-cast ingot was placed in an alumina crucible and heated under a vacuum to 1500 °C. After reaching 1500 °C, the growth chamber was backfilled with ultrahigh purity argon to a pressure of $2.76\times10^5$ Pa. Following pressurization, heating was continued until the ingot reached a temperature of 1600 °C and held for 1 h before being withdrawn from the furnace at a rate of 5 mm/hr. Following crystal growth, the ingot was annealed at 1000 °C for 168 h (using heating and cooling rates of 10 °C/min). Small parallelepipeds ($2\times1\times0.5$ mm$^3$) were cut from the ingot by wire electrical discharge machining and cleaned by acid etching and polished on one side. Samples were sealed in a quartz tube and annealed at 1000 °C for 4 h and furnace cooled down to room temperature. Composition measurements were done by energy-dispersive spectrometers in a JEOL 840A scanning electron microscope.

 

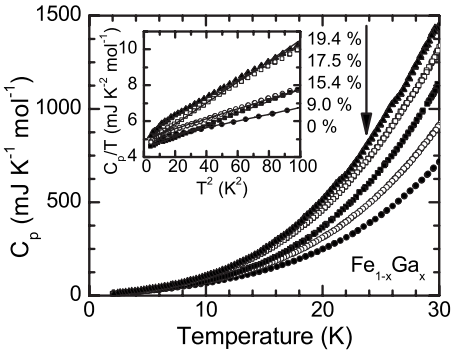


FIG. 1. Heat capacity $C_p$ versus temperature $T$ data for $Fe_{1-x}Ga_x$ alloys. The inset shows $C_p/T$ versus $T^2$ data (symbols) and linear fits (lines) over the range $T=2-10$ K.

## III. MEASUREMENTS

Heat capacity measurements were carried out using a Quantum Design physical property measurement system using a hybrid adiabatic relaxation technique.[10] The addenda were measured separately immediately before the sample measurement and subsequently subtracted. Heat capacity $C_p$ data for slow-cooled $Fe_{1-x}Ga_x$ alloys are shown in Fig. 1.

## IV. DATA ANALYSIS

At low $T$, the heat capacity for a soft ferromagnet is given by the formula

$$C_p = \gamma T + \beta T^3 + \alpha T^{3/2}, \tag{1}$$

where the terms represent the electronic, phonon, and spin-wave contributions, respectively. The spin-wave contribution of $\alpha$-Fe has been measured at very low temperatures and is estimated to be about a factor of 50 times smaller than $\beta$.[11–13] Our own analysis of the pure $\alpha$-Fe ($x=0$) data demonstrates that the heat capacity is not sensitive to the small spin-wave term proportional to $\alpha$ below 10 K. In this limit, the spin-wave term is ignored and the heat capacity can be written in the following form:

$$\frac{C_p}{T} = \gamma + \beta T^2. \tag{2}$$

The plot of the data as $C_p/T$ vs $T^2$ is shown in the inset of Fig. 1. The Sommerfeld constant ($y$ intercept) and lattice specific heat coefficient (slope) can then be obtained by a linear least-squares fit to the plot of $C_p/T$ vs $T^2$. To ensure close to linear behavior, the $C_p/T$ vs $T^2$ data were fitted over a low temperature range of 2–10 K. Error bars on the Debye temperatures were determined from variations in the fitted value for several different fitting ranges, as the statistical fitting errors were quite small. The parameters obtained from the fits are shown in Table I. The Debye temperature $\Theta_D$ can be derived from $\beta$ in the procedure described below and is also shown in Table I. The value obtained for $\gamma$ and $\Theta_D$ for pure $\alpha$-Fe are consistent with literature values.[14–19]

### A. Electronic heat capacity

Figure 2 shows that the electronic coefficient $\gamma$ remains essentially constant as the Ga concentration increases. At low temperatures, the electronic heat capacity is proportional to the DOS at the Fermi level $n(\varepsilon_F)$, according to the formula $\gamma = \frac{\pi^2}{3} R^2 n(\varepsilon_F)$, where $R$ is the universal gas constant.

TABLE I. Thermodynamic parameters obtained from fits by Eq. (2) to $C_p/T$ data.

| at. % Ga | $\gamma$ (mJ/mol K$^2$) | $\beta$ (mJ/mol K$^4$) | $\Theta_D$ (K) |
|---|---|---|---|
| 0.0 | 4.89(1) | 0.0187(1) | 470.2(8) |
| 9.0 | 5.03(1) | 0.0276(2) | 413(3) |
| 15.4 | 4.46(1) | 0.0332(1) | 388(3) |
| 17.5 | 4.69(1) | 0.0582(3) | 322 |
| 19.4 | 5.21(1) | 0.0521(2) | 334(4) |

To better understand our experimental results, we also performed density functional calculations for $Fe_{1-x}Ga_x$ alloys using the highly precise full-potential linearized augmented plane wave method.[20] No shape approximation is assumed for the charge, potential, and wave function expansions in the entire space. We used the generalized gradient approximation[21] for the description of the exchange correlation interaction. The convergence against parameters such as the number of **k** points and energy cutoff was carefully monitored. We used a $(2\times2\times2)$ supercell that comprises 16 atoms throughout the calculations, and we studied cases with $x=0.0$ (pure bcc $\alpha$-Fe), $x=0.0625$ ($Fe_{15}Ga_1$), $x=0.125$ ($Fe_{14}Ga_2$), and $x=0.1875$ ($Fe_{13}Ga_3$). For the $Fe_{14}Ga_2$ and $Fe_{13}Ga_3$ cells, there are several different ways to arrange Ga atoms on the bcc lattice sites due to different short-range ordered structures. Results reported below correspond to their minimum energy configurations. Figure 3 shows the calculated electronic DOS for $Fe_{1-x}Ga_x$ alloys with $x=0.0$, 0.0625, 0.125, and 0.1875, respectively. As $x$ increases, $n(\varepsilon_F)$

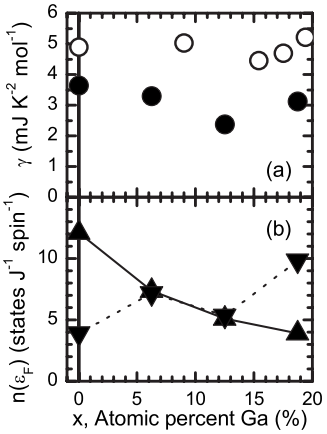


FIG. 2. (a) The electronic coefficient of the heat capacity ($\gamma$) of $Fe_{1-x}Ga_x$ alloys plotted as a function of Ga concentration $x$: experimental data (empty circles) and calculated (filled circles). In experimental data, the statistical error bars are smaller than the symbol size. (b) The spin-projected electronic density of states of majority (up triangles, solid line) and minority (down triangles, dotted line) spins at the Fermi level.

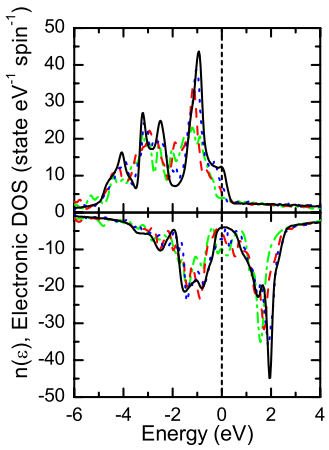


FIG. 3. (Color online) The calculated electronic density of states for $Fe_{1-x}Ga_x$ alloys with black solid lines for $x=0$ (i.e., pure bcc Fe), green dashed-dotted lines for $x=0.0625$, red dashed lines for $x=0.125$, and blue dotted line for $x=0.1875$. The positive side is for the majority spin channel, while the negative side is for the minority spin channel. Zero energy is the position of the Fermi level.

changes oppositely in the two spin channels. In the majority spin part, the Fe $d$ holes are gradually purged and $n_{\uparrow}(\varepsilon_F)$ falls monotonically. For $x \approx 0.125$, the Fe $d$ band in the majority spin channel is completely filled. Meanwhile, the number of nonbonding states around the Fermi level grows steadily in the minority spin channel. The trend of the $n(\varepsilon_F)$ versus $x$ curve reasonably matches with the experimental data of $\gamma$, as shown in Fig. 2. In the calculation, the small dip around $x \approx 0.125$ mainly stems from the elimination of the Fe majority spin $d$ holes due to the presence of Ga atoms. This dip feature is seen also in the experimental data; however, it is a small effect that is on the limit of the sensitivity of the technique.

### B. Lattice heat capacity

For a single, isotropic phonon mode with sound velocity $c$, the contribution to the low temperature molar heat capacity in the Debye model is

$$C_V = \frac{2\pi^2 R}{5}\frac{k_B^3 V}{\hbar^3 c^3}T^3, \tag{3}$$

where $V$ is the volume of the primitive cell, $R$ is the gas constant, and $\hbar$ is Planck's constant divided by $2\pi$. For a general cubic crystal with elastic anisotropy and three phonon polarizations, the form of the heat capacity is the same as Eq. (3), with $c$ replaced by the effective sound velocity $\bar{c}$, which is obtained by averaging the inverse-cubed sound velocities over all possible propagation directions and modes,

$$\frac{1}{\bar{c}^3} = \sum_i \int \frac{1}{v_i^3(\theta,\varphi)} d\Omega, \tag{4}$$

where $v_i(\theta,\varphi)$ is the sound velocity in a crystalline direction given by $\theta$, $\varphi$. The Debye temperature is defined as

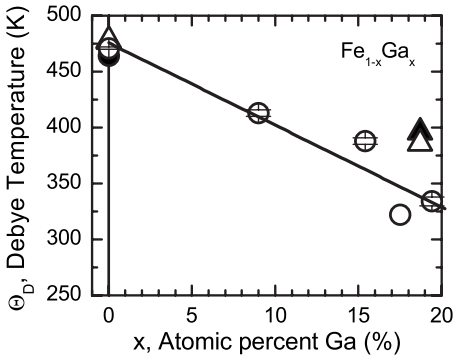


FIG. 4. The Debye temperature $\Theta_D$ plotted as a function of Ga concentration $x$ as determined from the data (empty circles). The solid line is a linear fit to the data. Various calculated $\Theta_D$ values are also shown, as determined from phonon density of states (filled circles), elastic constants (filled triangles), and the de Launay formula (empty triangles).

$$\Theta_D = \frac{\hbar \bar{c}}{k_B}\left(\frac{6\pi^2}{V}\right)^{1/3}, \tag{5}$$

such that the low temperature heat capacity can be written as

$$C_V = \frac{12\pi^4 R}{5}\frac{T^3}{\Theta_D^3} = \beta T^3 \tag{6}$$

and the slope of $C_V/T$ versus $T^2$ equals $\beta = (1943.9 \text{ J mol}^{-1} \text{ K}^{-1})\Theta_D^{-3}$. Experimentally determined values of $\Theta_D$ are given in Table I and are also shown in Fig. 4. $\Theta_D$ decreases approximately linearly with increasing Ga concentration, consistent with previous measurements of the tetragonal shear modulus $C'$ via resonant ultrasound[5] and neutron scattering.[7]

In an effort to affirm the validity of the measured Debye temperatures, we numerically calculated $\Theta_D$ via the two methods outlined below. These estimates of $\Theta_D$ are also shown in Fig. 4.

*(1) Integral.* The simplest way to calculate the Debye temperature from a lattice dynamical model is to calculate the heat capacity by integration. Given the model lattice dynamical parameters (obtained from fits to inelastic neutron scattering data, for example), the phonon density of states $g(E)$ can be calculated. The phonon DOS can then be used to calculate the heat capacity according to

$$C_V = 3R\int_0^{\infty} g(E)\left(\frac{E}{k_B T}\right)^2 \frac{e^{E/k_B T}}{[e^{E/k_B T}-1]^2} dE. \tag{7}$$

At low temperatures, the result of this calculation can be

fitted to the limiting form in Eq. (6) to obtain $\Theta_D$ in the same way as it was obtained from the measured data above. Figure 5(a) shows the calculated DOS for $\alpha$-Fe where the force constants are obtained by fitting the room temperature phonon dispersion curves measured by inelastic neutron scattering.[22] Using this DOS, we can calculate the heat capacity at low temperatures via Eq. (7) and, subsequently, fit the curve up to 10 K as shown in Fig. 5(b). The fitted slope, $1.94\times10^{-5}$ J mol$^{-1}$ K$^{-1}$, can then be used to obtain $\Theta_D$=464 K via Eq. (6).

*(2) Elastic constants.* Additionally, the Debye temperature can be calculated directly from the elastic constants. Any cubic system can be described by three independent elastic constants: $C_{11}$, $C_{12}$, and $C_{44}$. Generally these are experimentally measured as two transverse modes, $C_{44}$ (rhombohedral shear) and $C'=1/2(C_{11}-C_{12})$ (tetragonal shear), and one longitudinal mode, $K=1/3(C_{11}+2C_{12})$ (bulk modulus). Given these elastic constants, the sound velocities $\nu_i(\theta,\varphi)$ can be calculated for any propagation direction $(\theta,\varphi)$ using the Green-Cristoffel equations:

$$\begin{vmatrix} (C_{11}-C_{44})q_x^2+C_{44}q^2-\rho\omega^2 & (C_{12}+C_{44})q_xq_y & (C_{12}+C_{44})q_xq_z \\ (C_{12}+C_{44})q_yq_x & (C_{11}-C_{44})q_y^2+C_{44}q^2-\rho\omega^2 & (C_{12}+C_{44})q_yq_z \\ (C_{12}+C_{44})q_zq_x & (C_{12}+C_{44})q_zq_y & (C_{11}-C_{44})q_z^2+C_{44}q^2-\rho\omega^2 \end{vmatrix} = 0. \quad (8)$$

Solutions of Eq. (8) yield the sound velocities $\nu_i(\mathbf{q})=\omega_i(\mathbf{q})/q$ for each phonon branch along the crystal direction given by wave vector $\mathbf{q}$. The average sound velocity can then be evaluated for an anisotropic cubic crystal by numerical averaging as shown in Eq. (4). Subsequently, Eq. (5) can be used to calculate $\Theta_D$.

For $\alpha$-Fe, the zero-Kelvin elastic constants are extrapolated to be $C_{11}$=243.1 GPa, $C_{12}$=138.1 GPa, and $C_{44}$=121.9 GPa.[12] Calculation of the Debye temperature based on the above method gives $\Theta_D$=478 K, which compares favorably to the value determined from fits to the low temperature calorimetry data, as shown in Fig. 4. This can also be compared to the result obtained via the de Launay formula; a general semianalytic function to determine $\Theta_D(T)$ for cubic metals from the elastic constants.[23–25] Given the elastic constants listed above, this formula yields $\Theta_D(T=0\ \text{K})=477$ K.[12]

The elastic constants for quenched $Fe_{81.3}Ga_{18.7}$ were independently measured by Clark *et al.*[1] as a function of temperature. These were extrapolated to 0 K and substituted into the de Launay formula yielding $\Theta_D(T=0\ \text{K})=380$ K. They were also used via Eqs. (8), (4), and (5) to calculate $\Theta_D$=396 K. As can be seen in Fig. 4, these values are generally consistent with trends in the data.

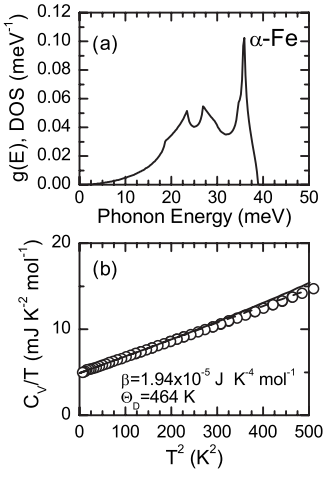


FIG. 5. (a) Phonon density of states $g(E)$ versus energy $E$ for $\alpha$-Fe as determined from a force constant model. (b) $C_V/T$ versus $T^2$ for the data (empty circles) and as calculated from Eq. (7) (solid line). The low temperature limiting slope (dashed line) gives a Debye temperature of 464 K.

## V. DISCUSSION

We find only a weak correlation between $\gamma$ and $\lambda_{100}$ with composition. Band structure calculations within density functional theory show that the small change in $\gamma$ is caused by the cancellation of two effects: a simultaneous depletion of holes in the majority spin band and the expected increase in $n_\downarrow(\varepsilon_F)$ in the minority band. Thus, while the heat capacity is not a sensitive probe of the relevant electronic states for magnetostriction in the case of $Fe_{1-x}Ga_x$, the agreement with band structure calculations is a positive step. The increase in $n(\varepsilon_F)$ after $x\gtrsim0.125$ manifests the presence of nonbonding states around the Fermi level in the minority spin channel. As revealed in our previous studies,[8] these states play a key role for the increase of $\lambda_{100}$, and the role of the effect of short-range ordering is an open question. Of course, more analyses on the details of wave functions, such as their magnetic quantum numbers, are needed for correct prediction. Results concerning the theoretical prediction of $\lambda_{100}$ will be published elsewhere.

In addition to the electronic behavior, the low temperature heat capacity can independently probe the lattice softening by determination of the Debye temperature. We find that the decrease of the Debye temperature agrees with previous estimates of lattice softening.

## VI. SUMMARY

We have measured the heat capacity as a function of temperature for $Fe_{1-x}Ga_x$, $0.0 < x < 0.194$ solid solutions crystallizing in the bcc structure. The Debye temperatures follow a linearly decreasing trend with increasing Ga concentration consistent with known lattice softening. The electronic coefficient of the specific heat remains relatively constant, in agreement with band structure calculations.

## ACKNOWLEDGMENTS

We thank S. Bud'ko and R. Rink for performing additional heat capacity measurements. R.W. also acknowledges support from the NSF (Grant No: DMR 0706503). Calculations were performed on supercomputers in the NERSC. Ames Laboratory is supported by the U.S. Department of Energy under Contract No. DE-AC02-07CH11358. This project is partially supported by the Office of Naval Research under ONR Grant No. N000140610530.

*mcqueeney@ameslab.gov

[1] A. E. Clark, K. B. Hathaway, M. Wun-Fogle, J. B. Restorff, T. A. Lograsso, V. M. Keppens, G. Petculescu, and R. A. Taylor, J. Appl. Phys. **93**, 8621 (2003).
[2] A. E. Clark, M. Wun-Fogle, J. B. Restorff, T. A. Lograsso, and J. R. Cullen, IEEE Trans. Magn. **37**, 2678 (2001).
[3] A. E. Clark, J. B. Restorff, M. Wun-Fogle, T. A. Lograsso, and D. L. Schlagel, IEEE Trans. Magn. **36**, 3238 (2000).
[4] G. Petculescu, K. B. Hathaway, T. A. Lograsso, M. Wun-Fogle, and A. E. Clark, J. Appl. Phys. **97**, 10M315 (2005).
[5] M. Wuttig, L. Dai, and J. Cullen, Appl. Phys. Lett. **80**, 1135 (2002).
[6] P. Mungsantisuk and S. Guruswamy, in *EPD Congress 2005: Proceedings of Sessions and Symposia held during the TMS Annual Meeting*, edited by M. E. Schlesinger (TMS, Warrendale, PA, 2005), pp. 193–198.
[7] J. L. Zarestky, V. O. Garlea, T. A. Lograsso, D. L. Schlagel, and C. Stassis, Phys. Rev. B **72**, 180408(R) (2005).
[8] R. Wu, J. Appl. Phys. **91**, 7358 (2002).
[9] L. Berger, Physica B & C **91**, 31 (1977).
[10] J. C. Lashley *et al.*, Cryogenics **43**, 369 (2003).
[11] M. Hatherly, K. Hirakawa, R. D. Lowe, J. F. Mallett, M. W. Stringfellow, and B. H. Torrie, J. Appl. Phys. **35**, 802 (1964).
[12] J. A. Rayne and B. S. Chandrasekhar, Phys. Rev. **122**, 1714 (1961).
[13] P. S. Mahesh and B. Dayal, Phys. Rev. **143**, 443 (1966), and references cited therein.
[14] G. Duyckaerts, Physica (Amsterdam) **6**, 401 (1939).
[15] W. H. Keesom and B. Kurrelmeyer, Physica (Amsterdam) **6**, 633 (1939).
[16] M. Dixon, F. E. Hoare, T. M. Holden, and D. E. Moody, Proc. R. Soc. London, Ser. A **285**, 561 (1965).
[17] S. S. Shinozaki and A. Arrott, Phys. Rev. **152**, 611 (1966).
[18] M. B. Stearns, Landolt-Börnstein, New Series, Group III, Vol. 19, Pt. A (Springer-Verlag, Berlin, 1986), Chap. 1, p. 118.
[19] *American Institute of Physics Handbook*, 3rd ed., edited by D. E. Gray (McGraw-Hill, New York, 1972), Chap. 4, p. 115.
[20] E. Wimmer, H. Krakauer, M. Weinert, and A. J. Freeman, Phys. Rev. B **24**, 864 (1981).
[21] J. P. Perdew, K. Burke, and M. Ernzerhof, Phys. Rev. Lett. **77**, 3865 (1996).
[22] V. J. Minkiewicz, G. Shirane, and R. Nathans, Phys. Rev. **162**, 528 (1967).
[23] J. de Launay, Solid State Phys. **2**, 219 (1956).
[24] J. de Launay, J. Phys. Chem. **21**, 1975 (1953).
[25] J. de Launay, J. Phys. Chem. **22**, 1676 (1954).